PHYSICAL REVIEW LETTERS

Geometry of Crumpled Paper

Daniel L. Blair* and Arshad Kudrolli

Department of Physics, Clark University, Worcester, Massachusetts 01610, USA
(Received 18 December 2004; published 29 April 2005)

We measure the geometry of a crumpled sheet of paper with laser-aided topography and discuss its statistical properties. The curvature of an elastoplastic fold scales linearly with applied force. The curvature distribution follows an exponential form with regions of high curvature localized along ridges. The measured ridge length distribution is consistent with a hierarchical model for ridge breaking during crumpling. A large fraction of the ridges are observed to terminate without bifurcating, and the ridge network connectedness is not as complete as anticipated. The self-affinity of the surface is characterized by a Hurst exponent of 0.71 ± 0.01 in contrast with previous results.

A crumpled piece of paper is an interesting and overwhelmingly familiar example of a stress induced morphological transformation in thin sheets. As a sheet is deformed, the bending energy becomes localized and the resulting crumpled shape is often thought of as a network of connected linelike ridges. These characteristic topologies are found in a variety of objects ranging from biological systems to engineering applications—for example, polymerized vesicle membranes and crumple zones in automobile bodies. In all situations, the response of the material can vary from purely elastic deformations to elastoplastic depending on the applied stress. Much of the theory for crumpled membranes and shells focuses on either equilibrium transformations found in biology [1] or the elastic properties of macroscopic sheets [2,3]. A number of recent studies [4–7] treat the geometry of developable cones which form the geometrical foundation for structures found when elastic sheets are subjected to point deformations. However, few studies exist that directly explore the crumpled state when elastoplastic deformations occur.

Early experiments focused on the fractal dimension of the ball that circumscribes a flat sheet once crumpled [8]. The acoustic emission from sheets that have been crumpled and unfolded display power-law scaling in the distribution of click energies [9,10]. By postulating that the ridge lengths are proportional to the energy released in acoustic emission, the authors indirectly measured the ridge distribution. Moreover, the lack of direct surface measurements have left many fundamental questions unanswered.

In this Letter, we report new experiments designed to directly measure the geometry of crumpled paper using noninvasive, laser-aided topographical reconstruction. Large sheets of paper are crumpled to a ball of fixed radius and then unfolded to reveal the plastic deformations made by the crumpling process. The surfaces are scanned by a laser sheet and the coordinates of the surfaces are reconstructed. Thus, we directly access the local curvature of the sheet and measure the properties of the ridges and their structure. We also examine the curvature of a single fold as

a function of applied force to probe the elastic and plastic deformations which occur during crumpling.

A schematic of the experimental configuration is shown in Fig. 1(a). Three kinds of paper are used (see Table I). The papers are first crumpled to "spheres" of radius $R_c \approx 120$ mm and then unfolded to a partially flat state. The uncrumpling process consists of opening the sphere, taking care not to tear the sheet while also making sure that we do
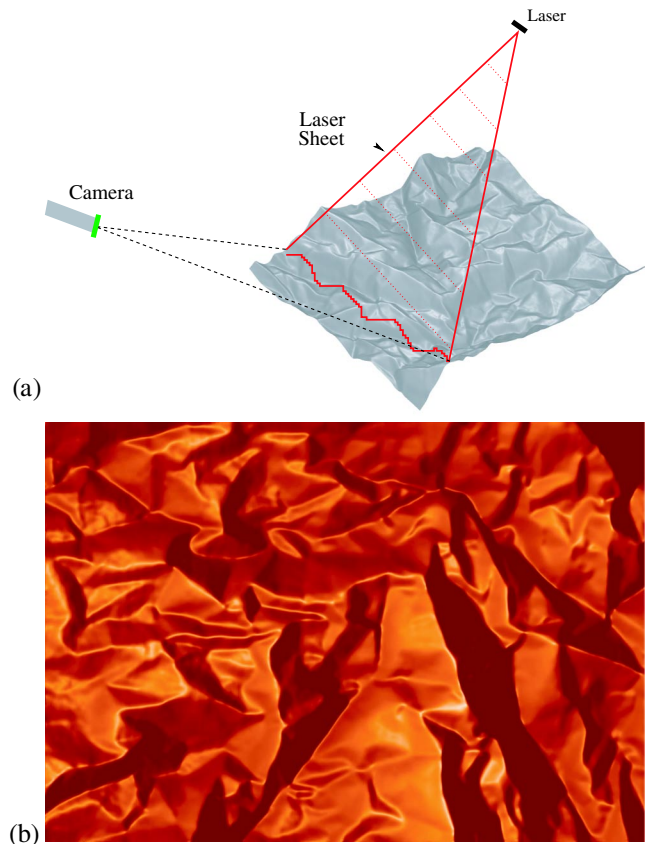

(a)

(b)

FIG. 1 (color online). (a) Schematic diagram of the experimental apparatus. (b) Example of a crumpled paper measured with laser-aided topography and rendered with shadow lighting.

TABLE I.   Mass, thickness, and size of paper used in the crumpling experiments.

Mass (g mm^{-2})	h_p (mm)	Size (mm × mm)
1.16×10^{-6}	0.156	560×610
1.89×10^{-6}	0.207	560×610
2.97×10^{-6}	0.360	430×355

not flatten the scars that are left on the paper. The opened sheets are then placed into the scanning setup for measurement. A laser with a cylindrical lens produces an approximately vertical sheet of light, and a CCD camera with a resolution of 1024×768 pixels captures the intersection of the light with the surface. When imaged from the side, the bright points, where the laser light intersects the surface, are proportional to the height [see Fig. 1(a)]. Each column of the image is first scanned for the highest pixel value, and that element is used for the brightness weighted centroid along that particular column. Care is taken to ensure that the laser light does not "disappear" behind structures. The laser sheet is rotated with a stepper motor which allows the entire surface to be scanned. After appropriate scaling and calibration, the crumpled surface is measured to within the thickness of the paper (see [11] for further details). An example of a crumpled surface is shown in Fig. 1(b), and corresponds to a 450 mm × 588 mm sheet of paper. The resulting "surface" is a matrix of elements whose value defines a height. Morphological features are extracted using a local quadratic fit to a local fitting region [12].

Before analyzing the entire crumpled surface, it is helpful to examine a single fold and the forces that cause them. Therefore, we folded a sheet of paper with thickness $h_p = 0.207$ mm, width $x = 150$ mm, and length $y = 588$ mm as shown in the inset of Fig. 2 about the center of the y axis (lengthwise). The two edges of the folded paper are affixed to the laboratory bench to prevent slipping, and then a known mass (force F) is placed across the length of the
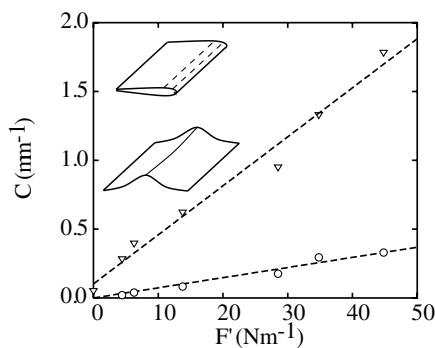
fold for uniform compression. After the mass is placed on the fold, the radius of the fold R_0 is directly measured. After approximately 30 s of waiting time, the mass is removed and the paper is unfolded and placed in the laser scanning apparatus. The inset of Fig. 2 shows schematically the resulting form of the unfolded sheet which is plastically deformed. A least squares fit to a circle centered at the apex of the fold yields the radius of curvature, R_f. It should be noted that the radii are measured on the outer surface and therefore include the thickness of the paper used. These measurements imply a lower bound on each measured radius, $R_{0,f} \gtrsim h_p$ where h_p is the paper thickness.

In Fig. 2 the initial and final curvatures C, (R_0^{-1}, R_f^{-1}) are plotted versus the force per unit length $F' = F/y$. As expected, the curvature of the fold increases with an increasing applied force. Interestingly, although there are always plastic deformations, the data are linear over 2 orders of magnitude in applied force. Furthermore, the time scales for the applied force in the hand crumpling and the single folding are equivalent, allowing for direct comparisons of the deformations.

We now turn to the analysis of fully crumpled sheets. The cross-sectional curvature c is defined as the plane that intersects with the plane of the slope normal, and perpendicular aspect direction. The distribution of the curvature magnitudes averaged in boxes of size 5 mm^2, $\bar{c}$, are shown in Fig. 3 for all h_p. Note that, as h_p increases, the high curvature tails also increase, indicating that for thicker sheets, plastic deformation is well preserved after uncrumpling. This result is expected by simply considering that the energy required to unfold a ridge must be proportional to h_p.

A proposed model of the distribution of energy in a crumpled sheet states that the process of crumpling forces the majority of the energy imparted to the sheet to be localized in a network of linelike ridges [9,13–16]. The
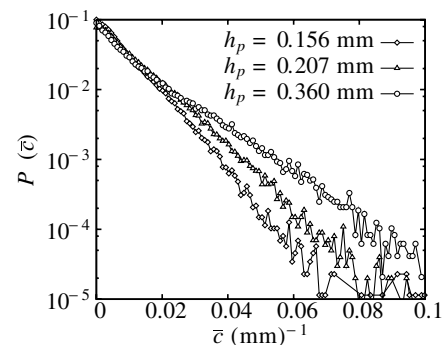

FIG. 2.   The curvature C of a folded sheet plotted versus F', the force per unit length. The shapes corresponding to the folded ($\triangledown$) and unfolded ($\bigcirc$) curvatures are shown in the inset.

FIG. 3.   The probability distribution of the magnitude of the curvature $P(\bar{c})$ averaged over regions of 25 mm^2 for each thickness of paper. The increase of the curvature for thicker sheets indicates that the uncrumpling process does not remove the quenched curvature of the ridges for thicker sheets.

structure of the ridge network is said to be that of a simple hierarchical structure. The structure is composed of large ridges that are randomly and unevenly "broken" into smaller ridges that produce a set of fragmented lengths. Therefore, a ridge of length ℓ should be equivalent to the original ridge length times a set of random variables that correspond to the fraction of ridge left after each breaking. The logarithm of the ridge lengths becomes a sum of random variables, i.e., a random walk. Therefore, the probability density function of the ridge length has the form, upon a change of variables back to lengths [16],

$$P(\ell) = \frac{1}{\sqrt{\pi}\sigma\ell} e^{-(\log\ell - \overline{\log\ell})^2/\sigma^2}, \tag{1}$$

a log-normal distribution with a ℓ^{-1} prefactor. To test this prediction, we measured the lengths of the ridges found in the hand crumpled sheets by identifying the points that lie along individual ridges via nearest neighbor criteria. We then perform a spline fit to each individual ridge and calculate the contour length of each spline. In Fig. 4 the distribution of ridge lengths are plotted for each h_p. The dashed line is a best fit to Eq. (1). To within experimental accuracy, the data are well described by this distribution function.

In theoretical treatments of crumpled surfaces, either equilibrium [1,17] or nonequilibrium [2,18,19], the structure of the surface is composed of randomly oriented ridges that always intersect at vertices to form a highly connected network. However, we observe that the *connectedness* of the network is not complete as anticipated. We also measure the number of neighbors that the "end" of a ridge will have, and find that many ridges do not intersect with other ridges. In Fig. 5(a), we plot the histogram of the number of nearest neighbors N_n, for 20 individual $h_p = 0.207$ mm sheets. The existence of ridges with zero nearest neighbors could have two explanations. Elastic deformations do not leave scars of the crumpling process. Therefore, the ridges that existed during crumpling do not appear when the sheet is unfolded. Second, the paper itself may be able to absorb the force that creates the ridge. The ridge may essentially
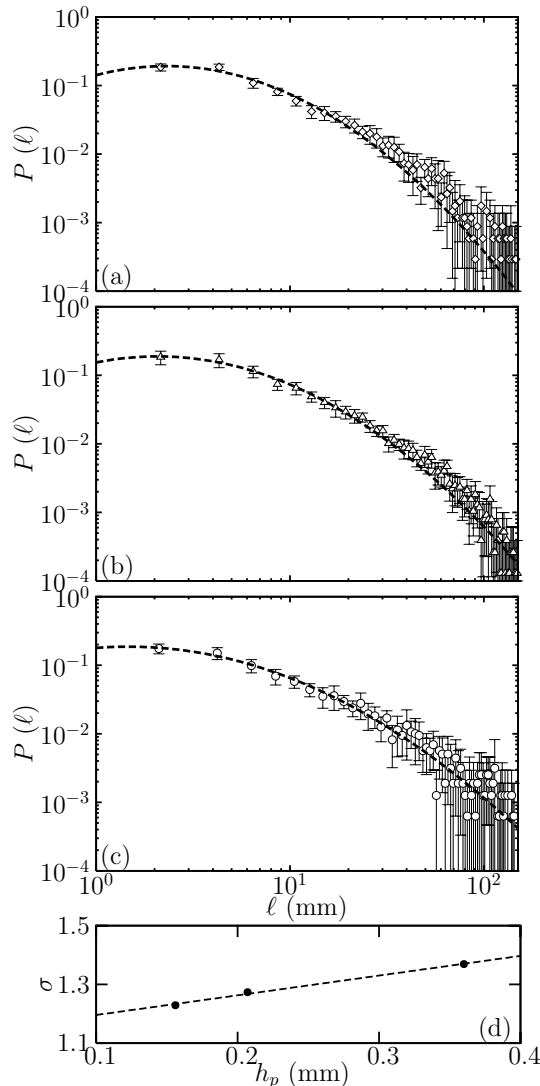

FIG. 4. The distribution of measured ridge lengths $P(\ell)$ (a) $h_p = 0.156$ mm, (b) $h_p = 0.207$ mm, and (c) $h_p = 0.360$ mm display. The dashed line is a fit to Eq. (1) and shows good agreement with and captures the existence of a peak. (d) Width of the log-normal distribution σ versus the paper thickness h_p, the dashed line is a linear least squares fit.
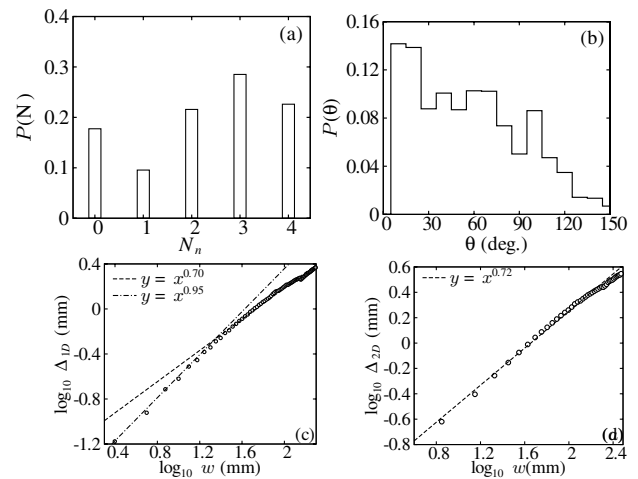

FIG. 5. (a) Histogram of the number of nearest neighbor ridges at a vertex N_n. The high frequency of zero occurrences indicates that many ridges dissipate into the paper. (b) Histogram of angle between ridges θ for $N_n = 3$. (c) Hurst plot of the one-dimensional line cross sections of the crumpled paper. The least squares fit gives the Hurst exponent H. We observe that for small w, there exists a scaling usually associated with $1/f$ noise and that for larger intervals the scaling follows $H \approx 0.70$. (d) Hurst plot of the two-dimensional crumpled gives $H \approx 0.72$. ($h_p = 0.207$ mm.)

dissipate at its edges due to the thickness of the paper itself. A question that may arise is if the sheet is crumpled "hard" enough. To answer this question, we note that squeezing the paper into a smaller R_c than used here often results in tearing which introduces new complications.

The angles that the ridges create with their neighbors is also measured. In Fig. 5(b) the histogram of the angles θ that are created by four ridges is plotted (i.e., the data in the $N_n = 3$ bin which correspond to single d cones), when they meet at a vertex. The values of θ appear broadly distributed in the range $0 \geq \theta \geq 180°$ indicating a somewhat random ordering. However, a number of predominant peaks at $\theta \leq 20°$, $\theta \approx 60°$, and $\theta \approx 110°$ are apparent. The existence of these peaks indicates that, indeed, the d-cone geometry dominates the intersection of ridges when $N_n = 3$, consistent with previous results [4,20]. However, the precise value of the predominant opening angle is still debatable.

Finally, to draw connections with previous experimental and theoretical studies of crumpled surfaces [21], we also performed surface scaling measurements. A self-affine surface $\zeta(x, y)$ is defined by the scaling of that surface by the transformation

$$x \to \lambda x, \qquad y \to \lambda y, \qquad \zeta \to \lambda^H \zeta, \qquad (2)$$

where λ is an arbitrary scaling factor and H is known as the Hurst exponent. In the case of a unbiased random walk $H = 0.5$, indicating no correlations. We measure H directly for each dimension using the following method. Each line scan is sectioned into nonoverlapping bins of width w that are increased in size until $w < L/2$, where L is the length of the scan. To ensure that we may consider each scan as statistically independent, we skip every ten scans. For each bin, the maximum difference between *elevations* within that bin Δ is recorded. This process is continued for each line, and the average of each interval is taken. For two dimensions the same process is used and the width w represents the linear dimension of the box where the maximum difference is measured. The relationship,

$$\log_{10}(\Delta) \propto H \log_{10}(w), \qquad (3)$$

directly gives the Hurst exponent. The one-dimensional Hurst plot [see Fig. 5(c)] demonstrates two distinct scaling regions. For intervals smaller than the characteristic ridge length, $H \approx 1.0$, indicating a planer geometry. In larger intervals, and for the two-dimensional analysis [see Fig. 5(d)], the scaling follows $H \approx 0.70$. These exponents indicate that our surfaces are not purely random, but demonstrate memory for distances greater than the average ridge length. Utilizing one-dimensional scanning profilometry of crumpled paper Plouraboué and Roux [21] have reported $H = 0.88$. We interpret the discrepancy as differences in experimental technique. Our laser based profilometry does not alter the surface of the uncrumpled sheets, which allows for more accurate measurements over all length scales.

In summary, we have examined the structure of a crumpled sheet of paper using laser-aided surface topography that allows for the complete reconstruction of the crumpled surface to unprecedented precision. While certain features such as ridge length distributions are found to be consistent with universal scaling laws, many subtleties are also revealed. A linear relationship between the applied stress and the resultant curvature of the plastic deformations implies that the surface curvatures can be mapped to the force distribution of crumpled surfaces. Because of the linearity of the response, a simpler theory may be possible to explain our observations. Additionally, we observe a considerable fraction of the ridges end without bifurcating.

　*Present Address: Department of Physics & DEAS, Harvard University, Cambridge, MA 02138, USA.

[1] D. Nelson, T. Piran, and S. Weinberg, *Statistical Mechanics of Membranes and Surfaces* (World Scientific, Singapore, 1988).

[2] E. M. Kramer and T. A. Witten, Phys. Rev. Lett. **78**, 1303 (1997).

[3] E. Cerda and L. Mahadevan, Phys. Rev. Lett. **90**, 074302 (2003).

[4] E. Cerda and L. Mahadevan, Phys. Rev. Lett. **80**, 2358 (1998).

[5] E. Cerda, S. Chaieb, F. Melo, and L. Mahadevan, Nature (London) **401**, 46 (1999).

[6] A. Boudaoud, P. Patrício, Y. Couder, and M. B. Amar, Nature (London) **407**, 718 (2000).

[7] E. Cerda, K. Ravi-Shankar, and L. Mahadevan, Nature (London) **419**, 579 (2002).

[8] M. A. Gomes, T. I. Jyh, I. M. Rodrigues, and C. B. S. Furtado, J. Phys. D **22**, 1217 (1989).

[9] E. M. Kramer and A. E. Lobkovsky, Phys. Rev. E **53**, 1465 (1996).

[10] P. A. Houle and J. P. Sethna, Phys. Rev. E **54**, 278 (1996).

[11] D. L. Blair, Ph.D. thesis, Clark University, 2004.

[12] J. Wood, Ph.D. thesis, University of Leicester, 1996.

[13] A. E. Lobkovsky, S. Gentges, H. Li, D. Morse, and T. A. Witten, Science **270**, 1482 (1995).

[14] A. E. Lobkovsky and T. A. Witten, Phys. Rev. E **55**, 1577 (1997).

[15] J. P. Sethna, K. A. Dahmen, and C. R. Meyers, Nature (London) **410**, 242 (2001).

[16] A. J. Wood, Physica (Amsterdam) **313A**, 83 (2002).

[17] Y. Kantor, M. Kardar, and D. R. Nelson, Phys. Rev. Lett. **57**, 791 (1986).

[18] M. A. F. Gomes, T. I. Jyh, and T. I. Ren, J. Phys. A **23**, L1281 (1990).

[19] B. A. DiDonna and T. A. Witten, Phys. Rev. Lett. **87**, 206105 (2001).

[20] S. Chaïeb, F. Melo, and J.-C. Géminard, Phys. Rev. Lett. **80**, 2354 (1998).

[21] F. Plouraboué and S. Roux, Physica (Amsterdam) **227A**, 173 (1996).